

# AlN Nanotubes: A DFT Study of Al-27 and N-14 Electric Field Gradient Tensors

Ahmad Seif<sup>a,b</sup>, Mahmoud Mirzaei<sup>c</sup>, Mehran Aghaie<sup>d</sup>, and Asadollah Boshra<sup>a,b</sup>

<sup>a</sup> Department of Chemistry, Boroujerd Branch, Islamic Azad University, Boroujerd, Iran

<sup>b</sup> Department of Chemistry, Science and Research Campus, Islamic Azad University, Tehran, Iran

<sup>c</sup> Department of Chemistry, Tarbiat Modares University, P.O. Box 14115-191, Tehran, Iran

<sup>d</sup> Faculty of Chemistry, North Tehran Branch, Islamic Azad University, Tehran, Iran

Reprint requests to M. M.; E-mail: mirzaei\_md@yahoo.com

Z. Naturforsch. **62a**, 711 – 715 (2007); received June 25, 2007

Density functional theory (DFT) calculations were performed to calculate the electric field gradient (EFG) tensors at the sites of aluminium ( $^{27}\text{Al}$ ) and nitrogen ( $^{14}\text{N}$ ) nuclei in an 1 nm of length (6,0) single-walled aluminium nitride nanotube (AlNNT) in three forms of the tubes, i. e. hydrogen-capped, aluminium-terminated and nitrogen-terminated as representatives of zigzag AlNNTs. At first, each form was optimized at the level of the Becke3, Lee-Yang-Parr (B3LYP) method, 6-311G\*\* basis set. After, the EFG tensors were calculated at the level of the B3LYP method, 6-311++G\*\* and individual gauge for localized orbitals (IGLO-II and IGLO-III) types of basis sets in each of the three optimized forms and were converted to experimentally measurable nuclear quadrupole resonance (NQR) parameters, i. e. quadrupole coupling constant ( $qcc$ ) and asymmetry parameter ( $\eta_Q$ ). The evaluated NQR parameters revealed that the considered model of AlNNT can be divided into four equivalent layers with similar electrostatic properties. With the exception of Al-1, all of the three other Al layers have almost the same properties, however, N layers show significant differences in the magnitudes of the NQR parameters in the length of the nanotube. Furthermore, the evaluated NQR parameters of Al-1 in the Al-terminated form and N-1 in the N-terminated form revealed the different roles of Al (base agent) and of N (acid agent) in AlNNT. All the calculations were carried out using the GAUSSIAN 98 package program.

*Key words:* Aluminium Nitride; Nanotube; DFT; NQR; Electric Field Gradient.

## 1. Introduction

Since the early days of the discovery and large scale production of carbon nanotubes (CNTs) [1, 2], numerous studies have been devoted on these novel materials. The applications of CNTs range from nanoelectronics to nanobiotechnology. For example, they are used as either electron field emitters or artificial muscles [3, 4]. However, since the electronic properties of CNTs are mainly dependent on the tubular chirality and diameter [5], separation of nanotubes with desired electronic properties from other ones is a formidable task. Therefore, substituting them by other non-carbon nanotubes with properties independent of these factors is an advantage for the production of desired nanotubes [6–8]. To this aim, elements of group III nitride nanotubes, e. g., boron nitride (BN) and aluminium nitride (AlN), are considered as possible and proper alternatives of CNTs [9, 10]. In contrast with CNTs, the group III nitrides are always wide gap semiconductors, the prop-

erties of which are independent of the tubular chirality and diameter, and among them, AlN has the largest band gap and is a good material for future electronics and optoelectronics [11, 12].

The formation of tubular BN structures in calculations and the first synthesized pure boron nitride nanotubes (BNNTs) were reported in [13, 14]. However, real aluminium nitride nanotubes (AlNNTs) have not been synthesized yet. Their stability and unique electronic properties were only indicated by theoretical studies [15–19]. Nuclear quadrupole resonance (NQR) spectroscopy, dealing with the quadrupole nuclei, is among the most versatile and insightful techniques to investigate the physical properties of matters [20]. The quadrupole nuclei are those with the nuclear spin angular momentum greater than one-half ( $I > 1/2$ ), e. g.,  $^{27}\text{Al}$  and  $^{14}\text{N}$ . From the measured NQR frequencies the quadrupole coupling constant ( $qcc$ ) and the asymmetry parameter ( $\eta_Q$ ) can be determined. The  $qcc$  is proportional to the interaction en-

ergy between the nuclear electric quadrupole moment ( $eQ$ ) and the electric field gradient (EFG) tensors at the sites of the quadrupole nuclei [21]. Another important measurable parameter is the asymmetry parameter ( $\eta_Q$ ), meaning the EFG tensors deviation from cylindrical symmetry at the sites of the quadrupole nuclei. The EFG tensors are very sensitive elements to the electrostatic environments and can reveal new trends about these properties in AlNNTs. Computationally, the EFG tensors calculated are proportional to  $q_{cc}$  and  $\eta_Q$ ; therefore, quantum chemical calculations permit the NQR measurable parameters evaluation [22, 23].

The present computational work studies the electrostatic properties of AlNNTs systematically. To this purpose, the EFG tensors are calculated to evaluate the  $^{27}\text{Al}$  and  $^{14}\text{N}$  NQR parameters ( $q_{cc}$  and  $\eta_Q$ ) (Tables 1, 2) as a first prediction for AlNNTs in a representative model of an 1-nm of length (6,0) single-walled AlNNT with hydrogen-capped, aluminium-terminated and nitrogen-terminated tubes (Figs. 1–4). The electrostatic properties of the terminating atoms are also specifically investigated by considering different tube models of AlNNTs.

## 2. Computational Procedure

In this work, an 1-nm of length (6,0) single-walled AlNNT, consisting of 24 Al and 24 N atoms, as the representative model of zigzag AlNNTs is studied in the three forms of tubes, i. e. H-capped, Al-terminated and N-terminated ones (Figs. 1–4). Density functional theory (DFT) calculations were performed on each of the three considered models by the GAUSSIAN 98 [24] package program. At first, geometrical optimization at the level of the Becke3, Lee-Yang-Parr (B3LYP) method and 6-311G\*\* basis set was performed on each of the three considered forms. Then, the EFG tensors at the sites of  $^{27}\text{Al}$  and  $^{14}\text{N}$  nuclei were calculated in each of the three optimized forms of H-capped, Al-terminated and N-terminated AlNNT (Figs. 2–4). The EFG tensor calculations were performed at the level of the B3LYP method, and 6-311++G\*\* and individual gauge for localized orbitals (IGLO-II and IGLO-III) types of basis sets to evaluate the  $^{27}\text{Al}$  and  $^{14}\text{N}$  NQR parameters,  $q_{cc}$  and  $\eta_Q$ , (Tables 1–2). There are five d-type Gaussian polarization functions on each non-hydrogen atom and three p-type polarization functions on each hydrogen atom in the large Pople's valence triple-zeta 6-311G\*\* and 6-311++G\*\* [25] basis sets in which the diffuse functions on all atoms indicated

by pluses are added to the latter one [26]. The larger Kutzelnigg's IGLO-II and IGLO-III [27] basis sets, having functions with large exponents for the representation of core electrons, are derived by Huzinaga's basis sets [28]. Both of 6-311++G\*\* and IGLO-types basis sets are adapted to reproduce reliable NQR and NMR properties [22, 23, 29, 30].

Since quantum chemical calculations do not directly yield the measurable NQR parameters ( $q_{cc}$  and  $\eta_Q$ ), (1) and (2) are used to evaluate  $q_{cc}$  and  $\eta_Q$ , respectively:

$$q_{cc}(\text{MHz}) = e^2 Q q_{zz} h^{-1}, \quad (1)$$

$$\eta_Q = |(q_{xx} - q_{yy})/q_{zz}|, \quad (2)$$

$$|q_{zz}| > |q_{yy}| > |q_{xx}|, 0 < \eta_Q < 1.$$

As mentioned earlier, the  $q_{cc}$  and  $\eta_Q$  can be determined by the measured NQR frequencies. The  $q_{cc}$  is proportional to the interaction energy between the  $eQ$  and the EFG tensors at the sites of quadrupole nuclei. The asymmetry parameter  $\eta_Q$  defines the EFG tensors deviation from cylindrical symmetry at the sites of quadrupole nuclei. The nuclei with the nuclear spin angular momentum greater than one-half ( $I > 1/2$ ) are quadrupoles. The standard  $Q$  values reported by Pyykkö [31] are employed in (1):  $Q(^{27}\text{Al}) = 146.6$  mb and  $Q(^{14}\text{N}) = 20.44$  mb. Tables 1 and 2 exhibit the evaluated NQR parameters at the sites of  $^{27}\text{Al}$  and  $^{14}\text{N}$  nuclei in the three considered forms of AlNNTs. Since the order of  $q_{cc}(^{27}\text{Al})$  is larger than that of  $q_{cc}(^{14}\text{N})$ , the values of  $q_{cc}(^{27}\text{Al})$  are reported by two digits and those of  $q_{cc}(^{14}\text{N})$  are reported by 3 digits, however, the values of  $\eta_Q$  for both,  $^{27}\text{Al}$  and  $^{14}\text{N}$ , are reported by two digits.

## 3. Results and Discussion

### 3.1. The $^{27}\text{Al}$ NQR Parameters

Table 1 exhibits the evaluated, experimentally measurable NQR parameters ( $q_{cc}$  and  $\eta_Q$ ) at the sites of  $^{27}\text{Al}$  nuclei in each of the three optimized H-capped, Al-terminated and N-terminated forms of the considered AlNNTs (Figs. 1–4). The evaluated NQR parameters reveal that the 24 Al atoms of the considered model can be divided into four equivalent layers with similar electrostatic properties in the length of the tube, Al-1, Al-2, Al-3 and Al-4 layers. The calculated parameters of the three employed basis sets agree with each other, and no significant differences are observed

Table 1. The  $^{27}\text{Al}$  NQR Parameters<sup>a</sup>.

Nucleus	$qcc$ (MHz)	$\eta_Q$
Al-1	40; 27; 40	0.12; 0.98; 0.15
	[39; 27; 39]	[0.14; 0.96; 0.16]
	(39; 27; 39)	(0.14; 0.96; 0.16)
Al-2	34; 33; 34	0.02; 0.06; 0.05
	[33; 32; 33]	[0.02; 0.06; 0.05]
	(33; 32; 33)	(0.02; 0.06; 0.05)
Al-3	34; 34; 34	0.04; 0.06; 0.08
	[33; 33; 33]	[0.04; 0.06; 0.08]
	(33; 33; 32)	(0.04; 0.06; 0.08)
Al-4	34; 34; 34	0.02; 0.02; 0.07
	[33; 33; 33]	[0.02; 0.02; 0.07]
	(32; 32; 33)	(0.03; 0.02; 0.08)

<sup>a</sup> In each row, the first number is for H-capped, the second one for Al-terminated and the third one for N-terminated forms of AlNNTs (see Figs. 2–4 for details). The results of the IGLO-II type basis set are in brackets, those of the IGLO-III type in parenthesis, and the others are for the 6-311++G\*\* basis set.

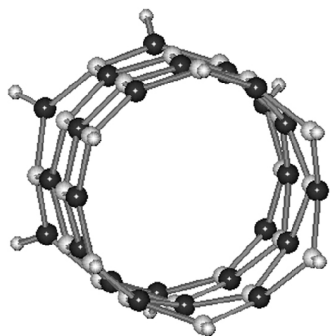


Fig. 1. 3D view of the (6,0) single-walled AlNNT.

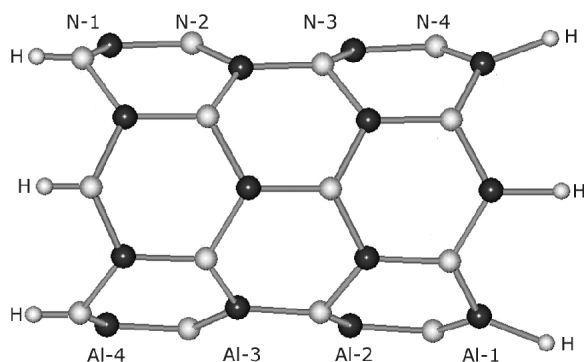


Fig. 2. 2D view of the H-capped form of the AlNNT.

with them, hence the magnitudes of the parameters are validated.

Al-1 layer is placed at the end of the tube and forms the Al end of the AlNNT. Therefore, because of the important roles of ending atoms in growing and synthesizing processes of nanotubes [32, 33], distinguished properties are expected for this layer. In both of the

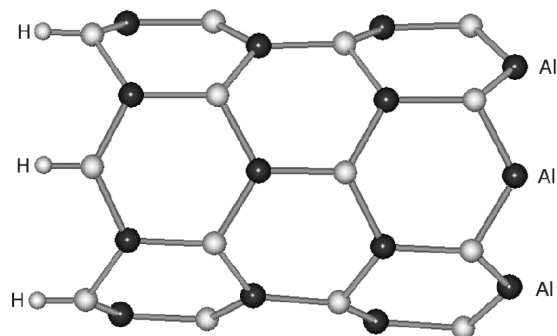


Fig. 3. 2D view of the Al-terminated form of the AlNNT.

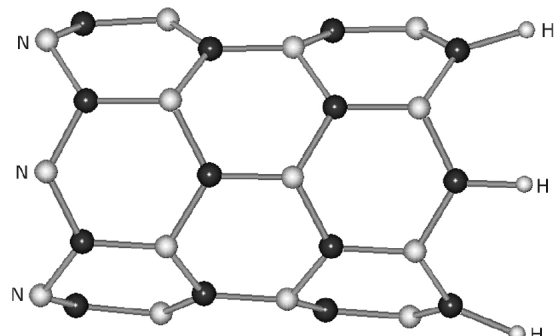


Fig. 4. 2D view of the N-terminated form of the AlNNT.

H-capped and N-terminated forms (Figs. 2 and 4),  $qcc(^{27}\text{Al-1})$  is 40 MHz, which means that this layer feels equivalent electrostatic environments in these two forms of AlNNTs. This trend reveals that the considered 1 nm of length AlNNT is a proper model to be studied because the different condition of the N-terminated form does not influence the electrostatic environment of the Al-1 layer. Furthermore, the magnitudes of  $\eta_Q(^{27}\text{Al-1})$  do not show any significant differences in the two considered forms of H-capped and N-terminated AlNNTs. However, the situation of the Al-1 layer in the Al-terminated form of an AlNNT is remarkably different from those with the H-capped and N-terminated forms.  $qcc(^{27}\text{Al-1})$  reduces by 13 MHz and  $\eta_Q(^{27}\text{Al-1})$  increases by 0.76 from the H-capped to the Al-terminated form, which means that the EFG tensors at the site of  $^{27}\text{Al-1}$  nuclei change significantly because of the Al-terminating situation. Al plays the base agent in an AlNNT, therefore, in the Al-terminated form, it has a better condition to interact with acid agents rather than those of H-capped and N-terminated forms.

Al-2, Al-3 and Al-4 layers are the other equivalent Al layers in the length of tube, for which the calcu-

Table 2. The  $^{14}\text{N}$  NQR Parameters<sup>a</sup>.

Nucleus	$qcc$ (MHz)	$\eta_Q$
N-1	2.29; 2.30; 8.00 [2.33; 2.34; 8.10] (2.32; 2.32; 8.12)	0.78; 0.78; 0.22 [0.76; 0.76; 0.21] (0.76; 0.76; 0.21)
N-2	0.55; 0.53; 1.02 [0.54; 0.52; 0.99] (0.53; 0.52; 1.02)	0.03; 0.05; 0.08 [0.01; 0.08; 0.07] (0.02; 0.07; 0.09)
N-3	0.51; 0.65; 0.52 [0.50; 0.63; 0.49] (0.50; 0.64; 0.51)	0.24; 0.29; 0.30 [0.28; 0.26; 0.37] (0.27; 0.28; 0.35)
N-4	0.90; 0.24; 0.88 [0.88; 0.27; 0.86] (0.90; 0.26; 0.89)	0.65; 0.53; 0.61 [0.67; 0.56; 0.66] (0.68; 0.57; 0.67)

<sup>a</sup> In each row, the first number is for H-capped, the second one for Al-terminated and the third one for N-terminated forms of AlNNTs (see Figs. 2–4 for details). The results of the IGLO-II type basis set are in brackets, those of the IGLO-III type in parenthesis, and the others are for the 6-311++G\*\* basis set.

lations (6-311++G\*\*) yielded an equal magnitude of 34 MHz for all of them. This trend reveals that in the considered AlNNT, the Al-1 layer plays a remarkable role in the Al layers as is easily seen by the equal calculated  $qcc$ 's of Al-2, Al-3 and Al-4 layers. Furthermore, just  $\eta_Q(^{27}\text{Al-1})$  has the significant difference comparing with  $\eta_Q$  of the other three Al layers Al-2, Al-3 and Al-4.

### 3.2. The $^{14}\text{N}$ NQR Parameters

The evaluated NQR parameters ( $qcc$  and  $\eta_Q$ ) from the calculated EFG tensors at the sites of  $^{14}\text{N}$  nuclei in the three optimized H-capped, Al-terminated and N-terminated forms of the considered AlNNTs (Figs. 1–4) are presented in Table 2. Parallel with the Al atoms, the 24 N atoms of the considered model can be divided into four equivalent layers with similar electrostatic properties, N-1, N-2, N-3 and N-4, according to their evaluated NQR parameters. The three employed basis sets of 6-311++G\*\*, IGLO-II and IGLO-III types yield no significant difference in the calculated results of Table 2 agrees with Table 1.

N-1 layer is placed at the end of the tube and makes the N end of the AlNNT. The magnitudes of  $qcc(^{14}\text{N-1})$  and  $\eta_Q(^{14}\text{N-1})$  in the two forms of H-capped and Al-terminated AlNNTs are almost the same; this means that removing H atoms in the Al-terminated form does not influence the electrostatic environment at the sites of N-1 nuclei. This trend reveals that parallel with Al-1, the considered length of the nanotube in the calculations is proper to study the electrostatic environment at the sites of ending  $^{14}\text{N}$

nuclei. However, when H atoms are removed in the N-terminated form, the evaluated NQR parameters of N-1 significantly deviate from the H-capped and Al-terminated forms.  $qcc(^{14}\text{N-1})$  increases by 0.7 MHz and  $\eta_Q(^{14}\text{N-1})$  reduces 0.56 from the H-capped to the N-terminated form. As mentioned earlier, Al plays as base agent in AlNNTs, and here N plays as acid agent from which the H atoms are removed; N-1 nuclei are more activated to interact with other base agents. In contrast with Al-1 layers the Al-2, Al-3 and Al-4 show almost similar properties in the three forms of AlNNTs, N-2, N-3, and N-4 layers do not show this similarity.

Although N-2 and N-3 layers have similar NQR parameters in the H-capped form, significant differences are seen in the two other forms. Since N has a lone pair of electrons, its electrostatic environment at the site of a nucleus is very sensitive and feels changes by the neighbouring effects which is easily observed by different NQR parameters of N-2 and N-3 in both the Al- and N-terminated forms of AlNNTs. The N-4 layer is the last one in the considered model of AlNNTs. The calculated magnitudes of  $qcc(^{14}\text{N-4})$  and also  $\eta_Q(^{14}\text{N-4})$  in H-capped and N-terminated forms are the same, meaning that removing the H cap in the N-terminated form does not influence the electrostatic environment at the sites of the N-4 nuclei. However, removing the H cap in the Al-terminated form causes significant changes in the calculated NQR parameters of N-4 which is the first neighbour layer of Al-1,  $qcc(^{14}\text{N-4})$  reduces by 0.65 MHz and  $\eta_Q(^{14}\text{N-4})$  reduces by 0.1 from the H-capped to the Al-terminated form.

## 4. Concluding Remarks

We performed a DFT study to evaluate NQR parameters ( $qcc$  and  $\eta_Q$ ) in a representative model of zigzag AlNNTs by calculations of EFG tensors at the sites of  $^{27}\text{Al}$  and  $^{14}\text{N}$  nuclei in three forms of tubes, i. e. H-capped, Al-terminated and N-terminated, for the first time. From the calculated results, some trends are concluded. First, the electrostatic environment at the sites of various nuclei in the considered model can be divided into four equivalent layers. Second, the NQR parameters at the sites of Al and N nuclei in ending layers (Al-1 and N-1) are significantly different from those of other layers, this trend being in agreement with the previous trends about the important roles of ending nuclei in nanotubes. The basic role

of Al and the acidic role of N are clearly observed in Al-terminated and N-terminated forms, respectively. Third, neighbouring with the N-1 layer does not influence the NQR parameters of Al-4 nuclei in the N-terminated form, however, the NQR parameters of N-4 nuclei are influenced in the Al-terminated form. Forth, except for Al-1 nuclei, the other three layers have equal magnitudes of NQR parameters, however, all of the

four N layers have different magnitudes of NQR parameters. Fifth, the NQR parameters of the central layers (Al-3 and N-3) can be extended to long AINNT systems. Sixth, good agreement in the calculated NQR parameters at the level of the employed 6-311++G\*\* and IGLO-type basis sets reveals that 6-311++G\*\* is large enough to reproduce reliable NQR parameters in AINNTs.

- [1] S. Iijima, *Nature* **354**, 2148 (1991).
- [2] T. W. Ebbesen and P. M. Ajayan, *Nature* **358**, 220 (1992).
- [3] O. Zhou, H. Shimoda, B. Gao, S. Oh, L. Fleming, and G. Yue, *Acc. Chem. Res.* **35**, 1045 (2002).
- [4] R. H. Baughman, C. Cui, A. A. Zakhidov, Z. Iqbal, J. N. Barisci, G. M. Spinks, G. G. Wallace, A. Mazzoldi, D. De Rossi, A. G. Rinzler, O. Jaschinski, S. Roth, and M. Kertesz, *Science* **284**, 1340 (1999).
- [5] P. J. F. Harris, *Carbon Nanotubes and Related Structures*, Cambridge University Press, Cambridge 1999.
- [6] J. Goldberger, R. He, Y. Zhangs, S. Lee, H. Yan, H. Choi, and P. Yang, *Nature* **422**, 599 (2003).
- [7] Q. Wu, Z. Hu, X. Wang, Y. Lu, X. Chen, H. Xu, and Y. Chen, *J. Am. Chem. Soc.* **125**, 10176 (2003).
- [8] V. N. Tondare, C. Balasubramanian, S. V. Shende, D. S. Joag, V. P. Godbole, S. V. Bhorasker, and M. Bhadhade, *Appl. Phys. Lett.* **80**, 4813 (2002).
- [9] A. Loiseau, F. Willaime, N. Demoncy, N. Schramchecko, G. Hug, C. Colliex, and H. Pascard, *Carbon* **36**, 743 (1998).
- [10] X. Chen, J. Ma, Z. Hu, Q. Wu, and Y. Chen, *J. Am. Chem. Soc.* **127**, 17144 (2005).
- [11] X. Balasé, A. Rubio, S. G. Louie, and M. L. Cohen, *Europhys. Lett.* **28**, 335 (1994).
- [12] I. Vurgaftman and J. R. Meyer, *J. Appl. Phys.* **94**, 3575 (2003).
- [13] A. Rubio, J. L. Corkill, and M. L. Cohen, *Phys. Rev. B* **49**, 5081 (1994).
- [14] N. G. Chopra, R. J. Luyken, K. Cherrey, V. H. Crespi, M. L. Cohen, S. G. Louie, and A. Zettl, *Science* **269**, 966 (1995).
- [15] S. Hou, J. Zhang, Z. Shen, X. Zhao, and Z. Xue, *Physica E* **27**, 45 (2005).
- [16] M. Zhao, Y. Xia, Z. Tan, X. Liu, F. Li, B. Huang, Y. Ji, D. Zhang, and L. Mei, *Chem. Phys. Lett.* **389**, 160 (2004).
- [17] M. Linnolahti and T. A. Pakkanen, *Inorg. Chem.* **43**, 1184 (2004).
- [18] D. Zhang and R. Q. Zhang, *Chem. Phys. Lett.* **371**, 426 (2003).
- [19] M. Zhao, Y. Xia, D. Zhang, and L. Mei, *Phys. Rev. B* **68**, 5415 (2003).
- [20] T. P. Das and E. L. Han, *Nuclear Quadrupole Resonance Spectroscopy*, Academic Press, New York 1958.
- [21] W. C. Bailey, *Chem. Phys.* **252**, 57 (2000).
- [22] M. Mirzaei and N. L. Hadipour, *J. Phys. Chem. A* **110**, 4833 (2006).
- [23] M. Mirzaei, N. L. Hadipour, and M. R. Abolhassani, *Z. Naturforsch.* **62a**, 56 (2007).
- [24] M. J. Frisch, G. W. Trucks, H. B. Schlegel, P. M. W. Gill, B. G. Johnson, M. A. Robb, J. R. Cheeseman, T. Keith, G. A. Petersson, J. A. Montgomery, K. Raghavachari, M. A. Al-Laham, V. G. Zakrzewski, J. V. Ortiz, J. B. Foresman, J. Cioslowski, B. B. Stefanov, A. Nanayakkara, M. Challacombe, C. Y. Peng, P. Y. Ayala, W. Chen, M. W. Wong, J. L. Andres, E. S. Replogle, R. Gomperts, R. L. Martin, D. J. Fox, J. S. Binkey, D. J. Defrees, J. Baker, J. P. Stewart, M. Head-Gordon, C. Gonzalez, and J. A. Pople, *Gaussian 98 Revision A.7*, Gaussian, Inc., Pittsburgh, PA 1998.
- [25] R. Krishnan, J. S. Binkley, R. Seeger, and J. A. Pople, *J. Chem. Phys.* **72**, 650 (1980).
- [26] T. Clark, J. Chandrasekhar, and P. R. v. Schleyer, *J. Comp. Chem.* **4**, 294 (1983).
- [27] W. Kutzelnigg, U. Fleischer, and M. Schindler, *The IGLO-Method: Ab Initio Calculation and Interpretation of NMR Chemical Shifts and Magnetic Susceptibilities*, Vol. 23, Springer-Verlag, Heidelberg 1990.
- [28] S. Huzinaga, *J. Chem. Phys.* **42**, 1293 (1965).
- [29] M. Schindler and W. Kutzelnigg, *J. Am. Chem. Soc.* **105**, 1360 (1983).
- [30] U. Fleischer, W. Kutzelnigg, A. Bleiber, and J. Sauer, *J. Am. Chem. Soc.* **115**, 7833 (1993).
- [31] P. Pyykkö, *Mol. Phys.* **99**, 1617 (2001).
- [32] E. Bengu and L. D. Marks, *Phys. Rev. Lett.* **86**, 2385 (2001).
- [33] S. Hou, Z. Shen, J. Zhang, X. Zhao, and Z. Xue, *Chem. Phys. Lett.* **393**, 179 (2004).